

22-26 September, 1986

The Determination of the Complete Neutron Scattering
Law $S(\mathbf{k}, \omega)$ from Total Scattering Experiments
using Computed Tomography.

M W JOHNSON

Rutherford Appleton Laboratory
Chilton, Oxon, OX11 0QX

ABSTRACT

This paper describes how the considerable body of knowledge on image reconstruction from path integrals (computed tomography) may be applied to total, time-of-flight neutron scattering experiments (ie those involving no experimental energy analysis) to obtain the neutron scattering law $s(\mathbf{k}, \omega)$. It is possible that such reconstruction techniques may have wide application in the fields of neutron powder diffraction, amorphous scattering, liquids scattering and quasi-elastic incoherent scattering. The technique was first described by the author in reference [1] .

1 INTRODUCTION

In a time-of-flight neutron scattering experiment in which no energy analysis is performed the recorded intensity in a particular detector and time channel is related to a curved path integral over the \mathbf{k}, ω plane. Adjacent time channels from the same detector provide an integral over a neighbouring, parallel, curved path. Typical paths for a detector at a scattering angle (2θ) of 10° are shown in Fig.1a. Detectors at different scattering angles have different paths and those for 30° and 60° are shown in Fig.1b and 1c.

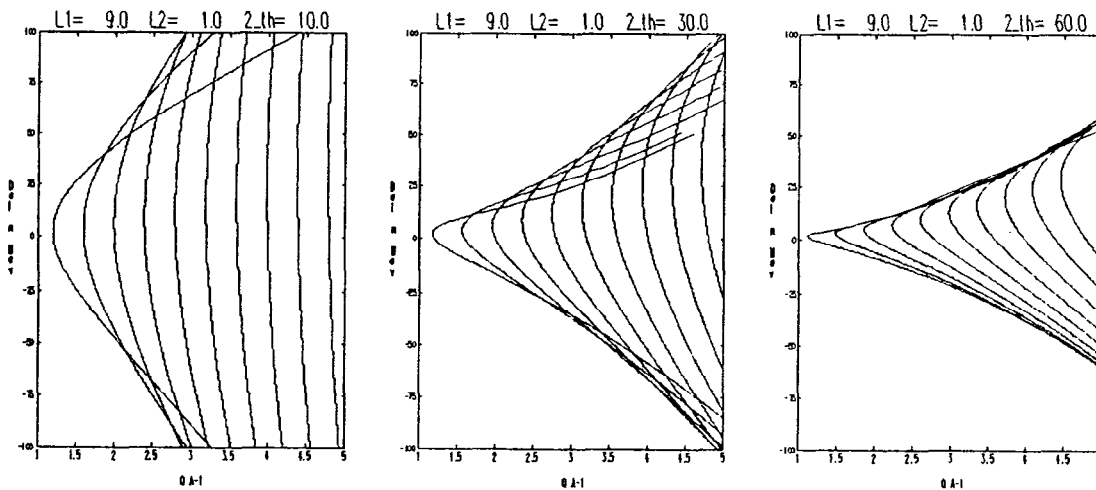


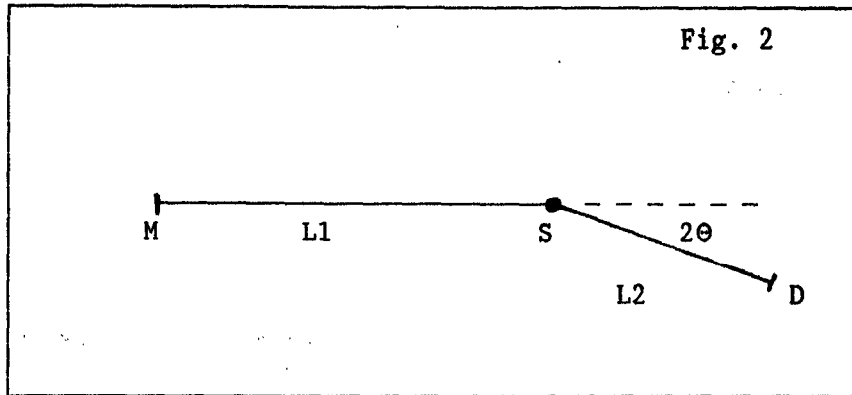
Fig 1

If the path integral can be written down in terms of a scattering law which is path-independent the problem may be mapped to the image reconstruction problem solved in real-space tomography.

In §2 we show how a total-scattering time-of-flight experiment may be expressed in a form suitable for reconstruction, and an example of a reconstruction is given in §3.

2 TOTAL NEUTRON SCATTERING

We consider an idealised time-of-flight neutron scattering experiment in which a pulsed, white beam of neutrons is incident on a sample (S) and detected (D) at a scattering angle of 2θ , Fig 2. All neutrons are assumed to leave the moderator (M) at time $t=0$.



Neutrons arriving at a time t at the detector may have been elastically or inelastically scattered, but their overall flight time determines a relationship between their primary and secondary energies E_1 and E_2 .

We have

$$t = t_1 + t_2 = \frac{m}{\hbar} \left(\frac{L_1}{k_1} + \frac{L_2}{k_2} \right) = \sqrt{\frac{m}{2}} \left(\frac{L_1}{\sqrt{E_1}} + \frac{L_2}{\sqrt{E_2}} \right) \quad - 2.1$$

Thus neutrons arriving at a particular time must have scattered from a point on a locus in the (E_1, E_2) plane defined by eq. 2.1.

More usefully we may describe this locus in the (κ, ω) plane where

$$\hbar\omega = E_1 - E_2 \quad - 2.2$$

$$\kappa = k_1 - k_2 \quad - 2.3$$

$$\kappa^2 = k_1^2 + k_2^2 - 2k_1k_2\cos(2\theta) \quad - 2.4$$

For any value of E_2 , E_1 is defined (eq. 2.1) and from these values $\hbar\omega$ and κ may readily be determined (eqs. 2.2, 2.4). The loci in the (κ, ω) plane are illustrated in Figs. 1a-1c.

The point of selecting the (κ, ω) plane is that, as a consequence of the first Born approximation to the cross section [2], all neutron scattering cross sections may be described in the form

$$\frac{d^2\sigma}{d\Omega dE_2} = \frac{k_2}{k_1} F(\kappa, \omega) \quad - 2.5$$

where $F(\kappa, \omega)$ is a function only of κ, ω and not k_1 or k_2 .

For example a monatomic liquid has:

$$F(\kappa, \omega) = \frac{N\sigma_c}{4\pi} S(\kappa, \omega) \quad - 2.6$$

Thus $F(\kappa, \omega)$ may be regarded as an 'image' in the κ, ω plane, which remains fixed when 'viewed' from differing angles. The different angles are provided by the varying loci corresponding to different $t, L1, L2$ combinations. The 'view' is obtained from the fact that the number of neutrons recorded in a particular time channel are related to an integral over a locus in the κ, ω plane.

The number of neutrons arriving per unit time $n(t)$ between times t and $t+\delta t$ in the idealised experiment shown above is given by:

$$n(t) = \int_{(\kappa, \omega) \text{ locus}} d\omega \frac{d^2\sigma}{d\Omega dE_2} \phi(E_1) \eta(E_2) \left(\frac{\partial E_1}{\partial t} \right)_{\omega} \quad - 2.7$$

$$= \int_{(\kappa, \omega) \text{ locus}} d\omega \frac{k_2 N \sigma_c}{k_1 4\pi} S(\kappa, \omega) \phi(E_1) \eta(E_2) \left(\frac{\partial E_1}{\partial t} \right)_{\omega} \quad - 2.8$$

a path integral over the (κ, ω) plane. Writing eq.2.8 in a discrete form we have

$$n_p = \sum_{i=1}^n \sum_{j=-m}^{+m} w_{ijp} S_{ij} \quad - 2.9$$

where S_{ij} is the value of $S(\kappa, \omega)$ in cell κ_i, ω_j in the κ, ω plane and w_{ijp} is a weight for that cell for path p . Note that we have chosen n κ cells ($i=1, n$) and $2m+1$ ω cells ($j=-m, \dots, 0, \dots, +m$) corresponding to the integral from $-\omega_{lim}$ to $+\omega_{lim}$

In the example of a monatomic liquid the weight would be:

$$w_{ijp} = \int_{(\kappa_i, \omega_j) \text{ cell}} d\omega \frac{k_2 N \sigma_c}{k_1 4\pi} \phi(E_1) \eta(E_2) \left(\frac{\partial E_1}{\partial t} \right)_{\omega} \quad - 2.10$$

We may further use the fact that the two halves of the κ, ω plane ($\omega < 0$ and $\omega \geq 0$) are related by the 'detailed balance' condition [2] :

$$S(\kappa, \omega) = \exp\{\hbar\omega/k_B T\} S(\kappa, -\omega) \quad - 2.11$$

Separating the equation 2.9 into two we may write:

$$n(t) = \sum_i \sum_{j=-m}^{j=-1} w_{ijp} S_{ij} + \sum_i \sum_{j=0}^{j=m} w_{ijp} S_{ij} \quad - 2.12$$

$$n(t) = \sum_i \sum_{j=0}^{j=m} (w_{ijp} + w_{i-jp} \exp\{-\hbar\omega_j/k_B T\}) S_{ij} \quad - 2.13$$

$$n(t) = \sum_i \sum_{j=0}^{j=m} w'_{ijp} S_{ij} \quad - 2.14$$

The inversion of the problem posed by eq.2.14 is completely analogous to the image reconstruction problem. A method of solution and references to similar problems is given in [1].

3 AN EXAMPLE

To illustrate the possibilities of this method the following steps were followed.

A discrete scattering law S_{ij} for an ideal gas was set up using a rectangular cell array on the κ, ω plane. Six ω cells spanned the region 0.0 to 50.0 meV, and 18 κ cells the range 1.0 to 5.0 Å⁻¹.

S_{ij} was calculated for the centre of each cell from the expression:

$$S(\kappa, \omega) = \frac{1}{\sqrt{4\pi\epsilon k_B T}} \exp\left\{-\frac{(\epsilon - \omega)^2}{4\epsilon k_B T}\right\}$$

where $\epsilon = \hbar^2 \kappa^2 / 2M$

A table of the values of S_{ij} thus produced is shown in Table a. Eighteen time of flight values were chosen for each of ten scattering

angles and their corresponding loci in (κ, ω) space computed (see Fig.1). The t -values at each scattering angle were chosen to cross the near centre of each elastic channel. The scattering angles were 10,20,30,40,50,60,70,80,90,100^o.

w_{ijp} were calculated for each path and the 180 path integrals computed from eqs. 2.10,2.13 with the assumption that the incident neutron spectrum, $\phi(E_1)$, followed that for an ambient moderator on the ISIS source [3]. The path integrals were then given random errors corresponding to fractional errors of $\sim 0.5\%$.

The reconstruction algorithm was then applied, using only the knowledge of the path integrals and their loci on the κ, ω plane.

Table 1b gives the values of the reconstructed S_{ij} values after 500,000 cycles ($\sim 30m$ cup for VAX8600). This shows remarkable agreement over the entire κ, ω plane and produces good estimates of the width (in ω) of the central peak feature and identifies the shift in its centre of gravity.

0.00	0.00	0.00	0.00	0.00	0.00	0.01	0.02	0.06	0.13	0.22	0.34	0.48	0.63	0.78	0.92	1.06	1.17
0.00	0.00	0.00	0.00	0.01	0.03	0.09	0.19	0.33	0.50	0.69	0.88	1.06	1.22	1.35	1.45	1.52	1.57
0.00	0.00	0.01	0.06	0.18	0.36	0.60	0.86	1.12	1.35	1.54	1.68	1.78	1.85	1.87	1.86	1.83	1.78
0.03	0.18	0.49	0.91	1.34	1.72	2.01	2.21	2.33	2.39	2.39	2.34	2.27	2.18	2.07	1.95	1.83	1.71
2.40	3.23	3.66	3.81	3.78	3.65	3.46	3.25	3.03	2.81	2.59	2.38	2.19	2.01	1.84	1.68	1.53	1.39
7.62	6.26	5.28	4.53	3.94	3.46	3.06	2.73	2.44	2.19	1.97	1.77	1.60	1.44	1.30	1.18	1.06	0.96

Table 1a

0.01	0.01	0.01	0.01	0.01	0.02	0.01	0.05	0.07	0.13	0.24	0.32	0.49	0.61	0.78	0.92	1.12	1.15
0.01	0.01	0.01	0.03	0.02	0.01	0.08	0.18	0.31	0.48	0.69	0.88	1.08	1.23	1.35	1.47	1.47	1.56
0.01	0.02	0.09	0.00	0.17	0.39	0.60	0.89	1.13	1.36	1.55	1.68	1.78	1.84	1.87	1.86	1.83	1.80
0.02	0.06	0.41	0.93	1.31	1.70	2.01	2.19	2.31	2.39	2.38	2.34	2.26	2.18	2.07	1.94	1.83	1.71
2.42	3.24	3.67	3.81	3.79	3.65	3.46	3.25	3.05	2.81	2.59	2.41	2.19	2.03	1.85	1.69	1.53	1.40
7.61	6.27	5.28	4.53	3.95	3.46	3.06	2.72	2.45	2.17	1.94	1.77	1.58	1.43	1.29	1.16	1.05	0.95

Table 1b

4 CONCLUSIONS

It is possible that the method described above may be of considerable use in separating elastic from quasi-elastic or inelastic scattering in neutron powder diffraction. If the k -range accessible to many detectors is sufficiently large the technique may be extended to liquids and amorphous problems and possibly the mapping of quasi-elastic incoherent cross sections.

REFERENCES

1. M.W.Johnson "The Determination of the Complete Neutron Scattering Law $S(Q,\omega)$ from Total Scattering Experiments using Computed Tomography." Rutherford Appleton Laboratory Report, RAL-86-041.
2. S.W.Lovesey "Theory of Neutron Scattering from Condensed Matter" Oxford University Press, Oxford ,1984.
3. A.D.Taylor "SNS Moderator Performance Predictions" Rutherford Appleton Laboratory Report, RAL-84-120.